STRUCTURAL-LOADS SURVEYS ON TWO TILT-WING VTOL CONFIGURATIONS

By John F. Ward

Langley Research Center

SUMMARY

The results of two structural-loads surveys are summarized. The first loads program discussed concerns the airframe vibratory loads encountered during flight tests of the VZ-2 tilt-wing VTOL aircraft throughout the operational range from hover to cruise flight. The primary sources of airframe vibration were wing-stall buffeting and tail buffeting in descents. The second loads program discussed concerns the initial results of a structural-loads survey conducted as part of the wind-tunnel test of a large-scale tilt-wing research model. This loads program deals with the steady wing loads measured throughout simulated transition from hover to cruise.

INTRODUCTION

This paper deals with the results of structural-loads surveys which were included as part of two of the VTOL research programs recently conducted at the Langley Research Center. These loads surveys were undertaken to investigate the nature of structural loadings associated with V/STOL aircraft incorporating the tilt-wing concept.

The first loads program that is discussed concerns the VZ-2 tilt-wing VTOL flight test aircraft. The principal result of this investigation was the determination of the character and relative magnitudes of vibratory loads that were encountered by the tilt-wing aircraft throughout the operational range from hover to cruise. Attention was focused on vibratory loads inasmuch as a number of limiting flight conditions were established, to a significant extent, on the basis of the severity of the airframe vibratory loads encountered.

The second loads program discussed concerns some of the initial results of a structural-loads survey conducted in conjunction with the wind-tunnel test of a large-scale, tilt-wing V/STOL model.

SYMBOLS

M	moment
M_{CRUISE}	steady bending moment in cruise (tunnel tests)
M_{HOVER}	steady bending moment in hover (tunnel tests)
M_{VIB}	vibratory bending moment (flight test)
$M_{STEADY,CRUISE}$	steady bending moment in cruise (flight test)
$M_{VIB,CRUISE}$	vibratory bending moment in cruise (flight test)
r	radial station
R	radius of rotor
V	free-stream velocity
α_w	wing angle of attack referenced to free-stream direction

L 1 4 3 2

FLIGHT INVESTIGATION OF VZ-2 AIRCRAFT

Test Procedures

Structural loads were monitored during the VZ-2 flying-qualities program at the Langley Research Center. This program included operation of the test-bed aircraft in the following flight conditions: hovering, transition, high-speed cruise, descents, and STOL operation. The program also included the investigation of the effects of a wing leading-edge modification installed to improve the aircraft behavior with regard to wing stalling limitations. With few exceptions, the flight program was conducted with incremental load factors less than $\frac{1}{4}g$, and rough-air conditions were avoided.

The airframe structural loads were monitored through the use of strain-gage bridges and a recording oscillograph. Figure 1 shows the test aircraft and the location of five strain-gage-bridge installations that will be referred to in this paper. In this figure the wing is shown in the hovering position. The locations of the strain-gage bridges used to monitor airframe vibratory loads are indicated in the figure; these gages measured horizontal- and vertical-tail bending moment, wing normal and chordwise bending moment, and wing-support-tube load. The main-rotor-blade flapwise vibratory bending moments were monitored by a strain-gage installation at the 48-percent blade radius.

Flight Results

Figure 2 illustrates some sample time histories of the output from the strain-gage installations shown in figure 1. These traces indicate the relative magnitude of airframe vibratory loads at three flight conditions. The wing angle of attack as given in this figure and used throughout this paper is defined as the angle between the wing-chord plane and the free airstream. The vibratory loads in the hover and cruise condition are of low magnitude. The condition shown for wing angle of attack of 60° was for a descent at 1,500 feet per minute. The buildup of vibratory load, in this case, was the maximum encountered in the flight program. The point illustrated is that the flight condition for maximum airframe vibratory load is the descent condition at high wing angles of attack. A 4.5-cycle-per-second frequency predominates in the traces for the vertical-tail bending, the wing support tubes, and the wing bending moment. From the relative deflection of the strain-gage traces and from the results of a simple ground check, this frequency appears to correspond to the fuselage torsional mode of vibration. The predominance of this mode is probably due to the fact that the large empennage is cantilevered from a rather flexible tubular fuselage.

The vibratory component of wing normal bending moment and vertical-tail bending moment is discussed in more detail so as to indicate the variation of airframe vibrations with wing angle of attack. Figure 3 presents the variation of the vibratory component of wing normal bending moment with wing angle of attack for level flight. The amplitude of the vibratory moments are referenced to a single value of the steady or mean wing normal moment measured in cruise. In the hover condition there is an increase in the magnitude of the wing vibratory load as the aircraft enters the ground-effect region. This region corresponds to wheel heights below approximately 20 feet. The effects of drooping the wing leading edge are indicated in the region of wing angle of attack of 30°. Without the drooped leading edge, wing-stall buffeting caused vibratory loads of 15 percent of the steady moment in cruise. After addition of wing-leading-edge droop the intensity of the vibratory loads induced by wing-stall buffeting reduced to 5 percent of the steady moment in cruise.

At stall onset the wing vibratory loads are induced by wing buffeting and are random in nature. At angles of attack above 40°, the wing vibratory loads, including the loads encountered in the ground-effect region, are primarily periodic at 4.5 cycles per second. The character of the vibratory loads at wing angles of attack above 40° indicates that the unsteady loads that are present are exciting the fuselage torsion mode of oscillation.

The buildup of the vibratory component of wing normal bending with rate of descent is presented in figure 4. The data in this figure and all subsequent figures for the VZ-2 aircraft were obtained with the drooped leading edge. The rate of descent is given in this figure to denote the flight condition in which the vibratory moment was encountered. The cut-off of the various curves at high wing angles of attack was due to the fact that unacceptable levels of pitch- and yaw-control roughness and airframe vibrations were encountered. The deterioration of pitch and yaw control suggests flow breakdown over the tail surfaces at high wing angles of attack and high rates of descent. In the descents the vibratory component of wing normal bending was periodic at 4.5 cycles per second just as was true in level flight at wing angles of attack above 40°.

Figure 5 illustrates the variation of vertical-tail vibratory load with wing angle of attack at various rates of descent. The vibratory component of vertical-tail bending moment is referenced to the magnitude of the vertical-tail vibratory moment measured in the steady cruise condition. As indicated in figure 5 there was a buildup of vertical-tail vibratory load in ground effect. The buildup of the vibratory load with rate of descent shows the same trend as the wing vibratory load presented in figure 4. The maximum values of vertical-tail vibratory loads were encountered at the limiting flight condition with unacceptable pitch and yaw control and airframe vibration. The character of the vibration was again a 4.5-cycle-per-second oscillation throughout the angle-of-attack range.

The large buildup of vertical-tail vibrations and the deterioration of pitch and yaw control at high wing angle of attack and high rates of descent suggest that the flow over the tail surfaces becomes increasingly unsteady and erratic as the descent rate increases for a given wing angle of attack. Figure 6 presents the buildup of tail vibratory load, at $\alpha_w = 60^{\circ}$, as a function of rate of descent. This figure is merely a cross plot of data from figure 5. A significant parameter which reflects the nature of the flow conditions in the descents is the rotor slipstream velocity. The calculated values of rotor slipstream velocity at the rates of descent investigated are indicated in this figure. The decreasing values of rotor slipstream velocity are a result of the reduced horsepower at the increased descent rates.

Figure 7 illustrates an estimate of the flow situation at the flight condition in which the maximum airframe vibrations were encountered. This situation corresponds to the end point on the curve of figure 6 with a wing angle of attack of 60°, rate of descent of 1,500 feet per minute, and a rotor slipstream velocity of 80 feet per second. The free-stream velocity for this flight condition was 70 feet per second.

The flow situation that develops at limiting rates of descent is the result of a number of contributing factors. A few of the more significant of these factors are suggested as follows. As the rotor slipstream velocity is decreased, the local wing angle of attack increases until stalling occurs. With the onset of stall, wing buffet loads develop so that airframe vibrations are induced. As the stalling spreads over the wing, the flow breakdown results in turbulence behind the wing-rotor combination. At the high wing angles of attack and high rates of descent, this turbulence is carried back over the tail surfaces inducing tail buffeting and loss of control effectiveness. The unsteady flow impinging on the tail surfaces contains a wide spectrum of input frequencies and therefore excites the fuselage mode at 4.5 cycles per second. There are many other factors contributing to the unsteady flow over the tail, such as fuselage interference, rotor slipstream turbulence, and engine-exhaust effects. These effects are probably secondary with respect to the flow breakdown induced by flying a stalled wing ahead of the tail during the descent.

L
1
4
3
2

Regardless of the details of the flow conditions which cause the airframe vibrations and control roughness that limit the rates of descent that may be achieved, the basic problem lies with the stalling and flow breakdown over the wing-rotor combination. This flow breakdown plays a dual role in introducing airframe vibrations and control roughness during descents. The direct effect of wing stall is reflected in wing buffeting loads at the onset of stall. The second and perhaps more significant effect takes place at higher wing angles of attack where the turbulent flow from the wing-rotor combination is carried back over the tail surfaces and leads to severe tail buffeting and deterioration of pitch and yaw control.

In the design of tilt-wing aircraft that are to be capable of achieving steep descents, it will be necessary to minimize the effects of wing stall, wing and rotor slipstream turbulence, and tail buffeting. Wing-stall onset can be delayed by employing high-lift devices such as slats and flaps. The effects of wing-rotor slipstream turbulence on tail buffeting can be minimized by properly locating the tail surfaces with respect to the path of the wing and rotor wake for the operational descent conditions. In this regard it will also be possible to draw upon the results of the research on tail buffeting already accomplished in connection with the development of the conventional airplane.

Up to this point, discussion has dealt with airframe vibrations in general. Figure 8 deals with the main-rotor-blade one-per-revolution vibratory moment variation with wing angle of attack in level flight. In this figure the magnitude of the blade flapwise bending moment is expressed as a ratio of the constant value of the blade vibratory moment measured in the cruise condition. As indicated in the figure, the magnitude of the one-per-revolution load increases to a maximum at

a wing angle of attack of 45°. This peak at an intermediate wing angle of attack is the result of the presence of relatively high free-stream dynamic pressure and unsymmetrical flow conditions at the rotor disk.

The VZ-2 loads survey indicated that the maximum airframe vibratory loads encountered occurred in descents at high wing angles of attack and were a result of tail buffeting induced by flow breakdown over the wing and rotor combination. Also, the maximum rotor-blade vibratory loads encountered occurred in level flight at intermediate wing angles of attack. These results suggest that, for the tilt-wing aircraft, the transition region between hover and cruise will require close attention in regard to fatigue-life substantiation.

TUNNEL-MODEL INVESTIGATION

This part of the discussion deals briefly with some of the initial results from the structural-loads survey conducted as part of the aerodynamic performance investigation of a large-scale tilt-wing V/STOL model. This investigation was conducted in the Langley full-scale tunnel. The complete results of the wind-tunnel investigation, which includes simulated accelerating and decelerating transition with various flap settings, are not presently available.

Test Procedures

The semispan of the configuration of the large-scale model is indicated in frontal view in figure 9 and in planform view in figure 10. The complete details of the configuration are given in reference 1, which presents results of ground effects on this same model. The wing structural loads were measured at the wing root with the strain-gage-bridge installation illustrated in figures 9 and 10. The strain-gage bridges were installed and calibrated according to the procedures outlined in reference 2. The wing loads measured included wing bending moment and shear in the normal and chordwise directions and wing torque. The outputs of these strain-gage bridges were monitored on a recording oscillograph throughout the wind-tunnel investigation.

Tunnel Test Results

Figures 9 and 10 illustrate the variation of the wing normal and chordwise bending moment through the angle-of-attack range from hover to cruise. These data are for unaccelerated transition with zero flap deflection. These loads are the steady moments due to aerodynamic loading on the wing during simulated steady-level-flight transition. The lift

was held constant throughout the transition and was equal to an aircraft weight of 3,500 pounds.

In general, the data indicate no abrupt change in spanwise centers of pressure. The shift of lift from the stalled wing to the propellers is indicated by the reduction in wing normal moment and the corresponding increase in chordwise moment at wing angle of attack of 45°. One other point is the presence of a wing normal moment in hover which is 30 percent of the value for cruise. This positive normal moment is due to the cambered wing acting in the high velocity propeller slipstream. To date no unusual structural loading problems have been noted, and it is expected that it will be possible to provide detailed structural-loads data for accelerating and decelerating flight throughout the transition range.

L
1
4
3
2

CONCLUSIONS

From a structural-loads survey of the tilt-wing VZ-2 aircraft in flight and preliminary results of a large-scale tilt-wing model in a wind tunnel, the following conclusions are indicated:

1. The flight-loads survey of the VZ-2 indicated that the primary sources of airframe vibratory loads are wing and tail buffeting. The vibratory loads result from wing buffeting at stall onset and from impingement of the separated flow from the stalled wing on the tail surfaces. The airframe vibratory loads encountered reached the maximum at high wing angles of attack during low-power descents with reduced rotor-slipstream velocities.

2. The addition of a leading-edge modification tended to reduce the intensity of the wing vibratory loads associated with the onset of wing-stall buffeting.

3. The rotor-blade one-per-revolution vibratory loads reached the maximum at intermediate wing angle of attack in consequence of the combination of relatively high free-stream dynamic pressure and unsymmetrical flow conditions at the rotor.

4. The initial wind-tunnel results of the structural loads survey of the large-scale tilt-wing model indicated no unusual behavior as regards the steady-wing loads during transition from hover to cruise.

REFERENCES

1. Huston, Robert J., and Winston, Matthew M.: Data From a Static-Thrust Investigation of a Large-Scale General Research VTOL-STOL Model in Ground Effect. NASA TN D-397, 1960.

2. Skopinski, T. H., Aiken, William S., and Huston, Wilber B.: Calibration of Strain-Gage Installations in Aircraft Structures for the Measurement of Flight Loads. NACA Rep. 1178, 1954. (Supersedes NACA TN 2993.)

VZ-2 STRAIN-GAGE INSTALLATION

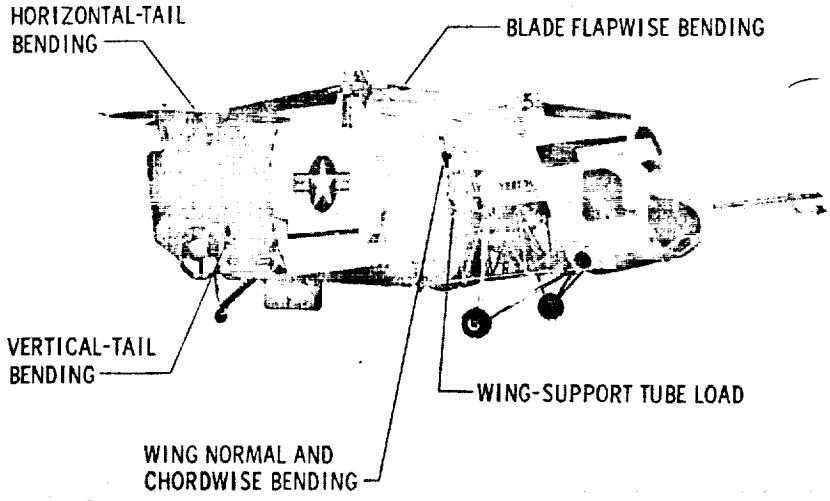

Figure 1

VZ-2 AIRFRAME VIBRATORY LOADS

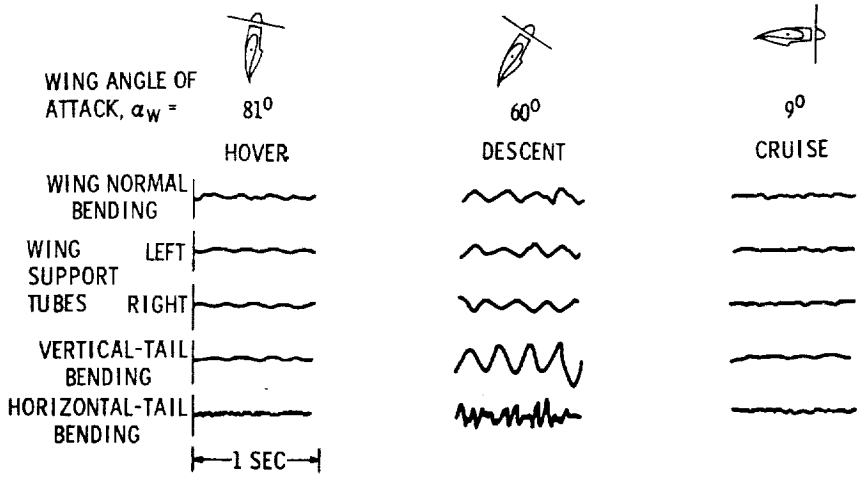

Figure 2

VIBRATORY COMPONENT OF WING NORMAL BENDING MOMENT

LEVEL FLIGHT

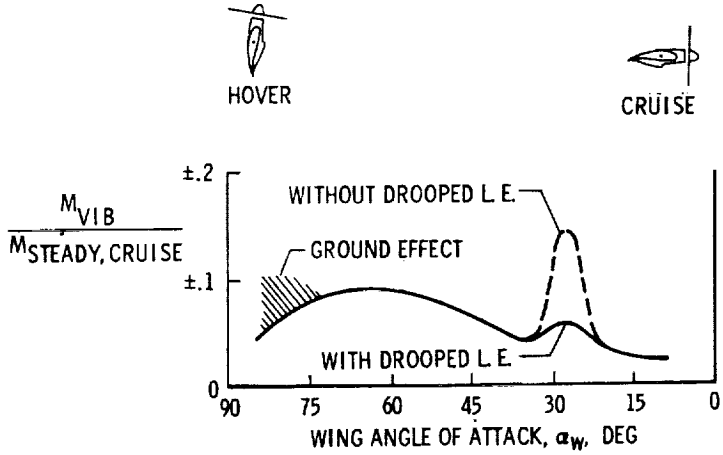

Figure 3

VIBRATORY COMPONENT OF WING NORMAL BENDING MOMENT

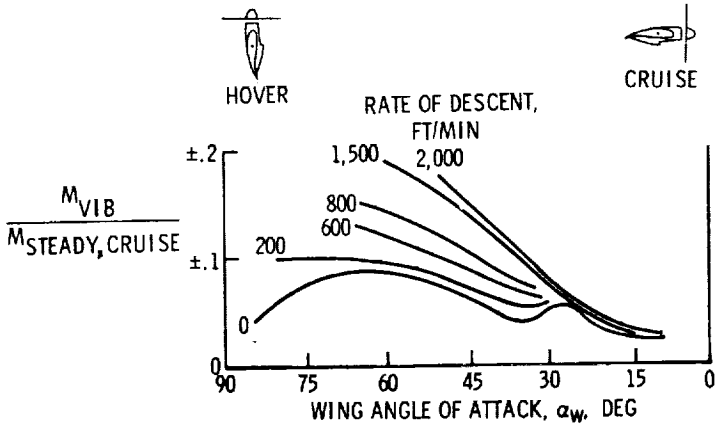

Figure 4

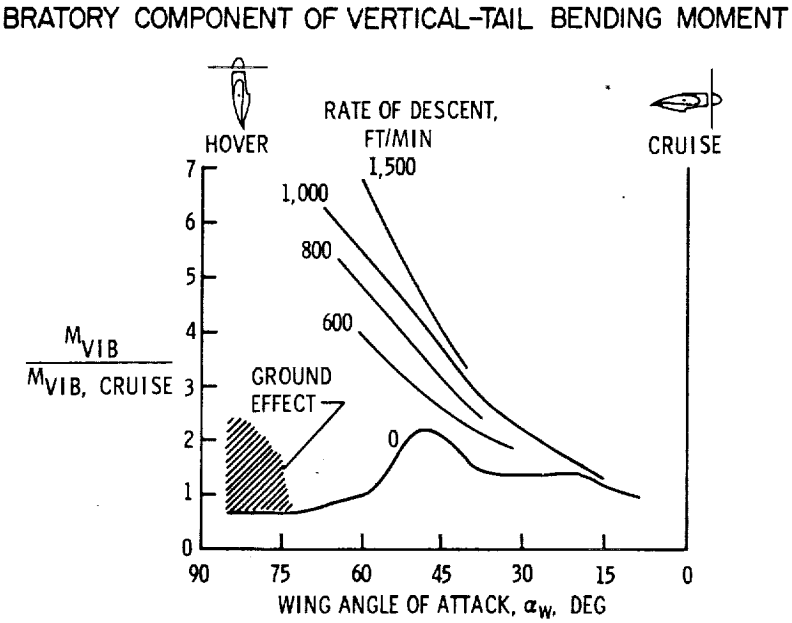

Figure 5

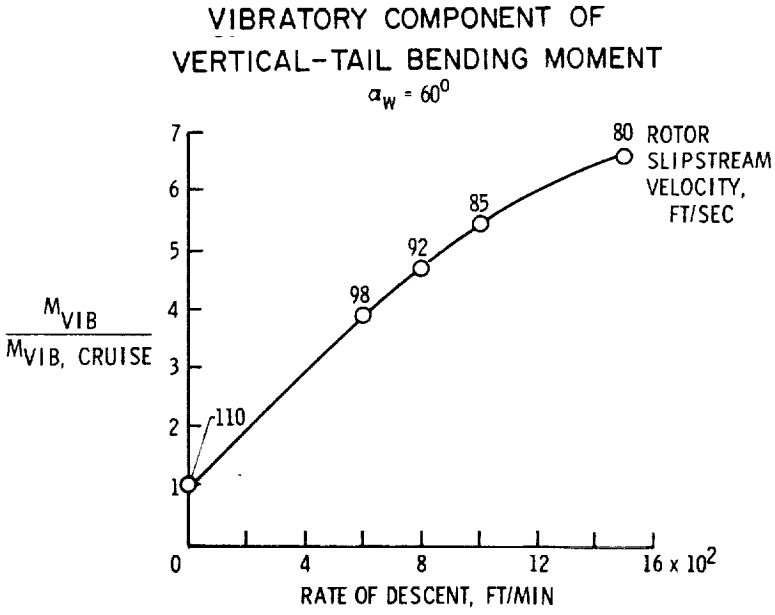

Figure 6

FLIGHT CONDITION FOR MAXIMUM AIRFRAME VIBRATORY LOADS

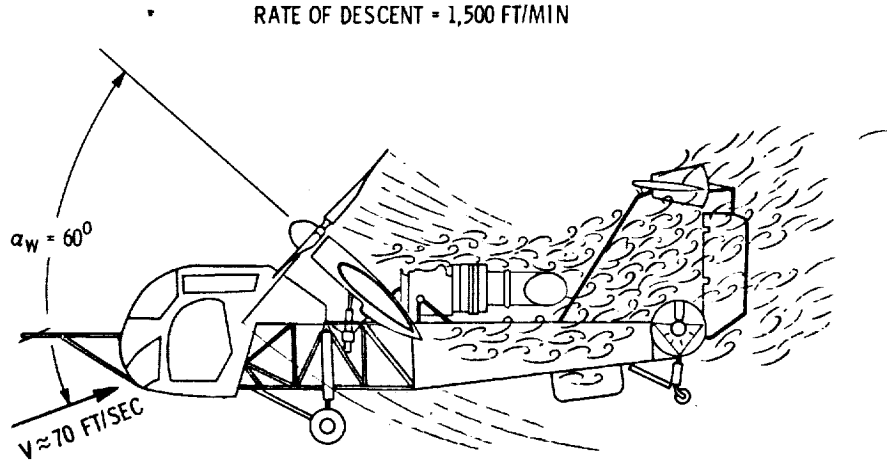

Figure 7

VIBRATORY COMPONENT OF MAIN-ROTOR BLADE FLAPWISE BENDING MOMENT

LEVEL FLIGHT

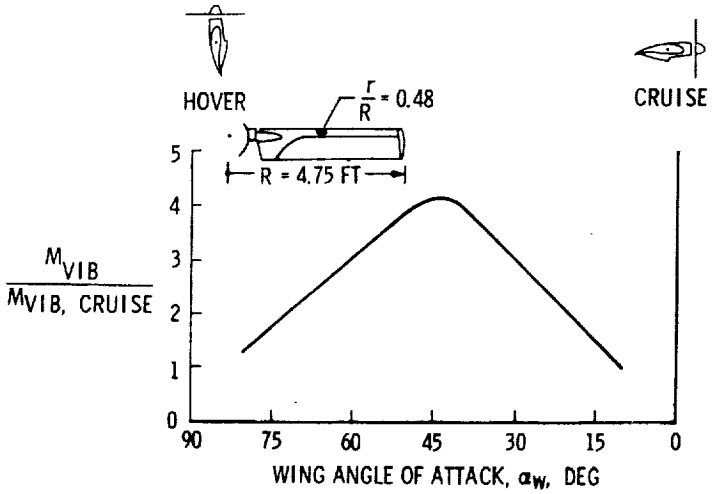

Figure 8

VARIATION OF WING NORMAL BENDING MOMENT DURING TRANSITION

STEADY LEVEL FLIGHT

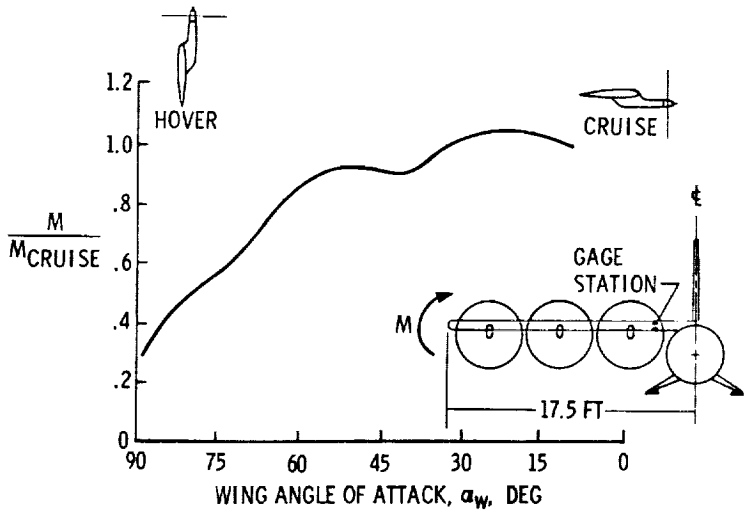

Figure 9

VARIATION OF WING CHORDWISE BENDING MOMENT DURING TRANSITION

STEADY LEVEL FLIGHT

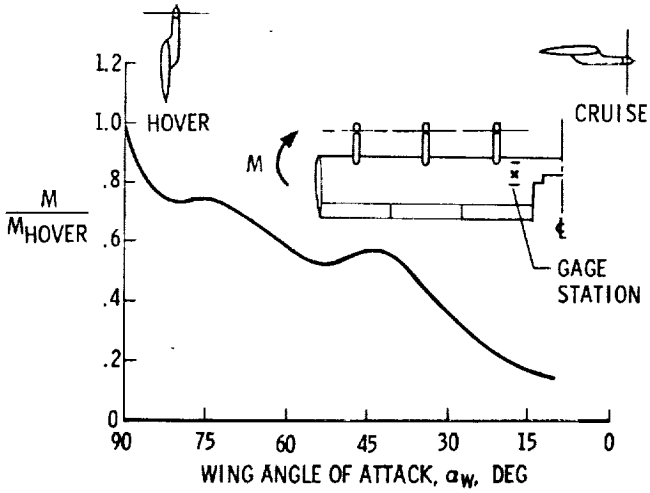

Figure 10